Research Article

대한치과재료학회지 53(3) : 133-148, 2026
Korean Journal of Dental Materials (*Korean J Dent Mater*)
ISSN:2384-4434 (Print); 2384-3268 (Online)
Available online at http://www.kadm.org
http://dx.doi.org/10.14815/kjdm.2026.53.3.133

조직유도재생을 위한 젠타마이신 함유 키토산/폴리비닐알코올 전기방사 이중기능성 나노섬유 지지체의 제조

박경희, 송요한, Alphonse Umugire, 한미경, 박영준*

전남대학교 치의학전문대학원 치과재료학교실

Fabrication of gentamicin-loaded chitosan/polyvinyl alcohol electrospun nanofibrous dual-functional scaffolds for guided tissue regeneration

*Kyung Hee Park, Yo-Han Song, Alphonse Umugire, Mi-Kyung Han, Yeong-Joon Park**

Department of Dental Materials, School of Dentistry,
Chonnam National University, Gwangju, Republic of Korea

본 연구에서는 조직유도재생(guided tissue regeneration, GTR)을 위한 다기능성 지지체로서 다양한 농도의 젠타마이신(gentamicin, Gm)을 함유한 키토산/폴리비닐알코올 (polyvinyl alcohol, PVA) 전기방사 나노섬유 매트의 조성 변화에 따른 영향을 평가하였다. 젠타마이신 함유 키토산/PVA 나노섬유(GmCP)의 형태학적 특성, 열적 안정성, 팽윤 거동, 기계적 특성, 항균 활성 및 세포적합성을 체계적으로 평가하였다. 젠타마이신의 첨가는 GmCP 나노섬유의 구조적 또는 열적 안정성에 영향을 미치지 않았다. 특히 Gm 용액의 함량을 1.0% (w/v)까지 증가시킴에 따라 인장강도, 영률(Young's modulus) 및 연신율이 향상되어 나노섬유 매트의 기계적 특성이 개선되었다. 이러한 향상은 PVA, 키토산 및 젠타마이신 사이의 분자 간 상호작용이 강화되었기 때문으로 판단된다. 팽윤율은 Gm 용액의 함량이 증가함에 따라 감소하였으며, 이는 가교밀도가 증가하였음을 시사한다. GmCP 나노섬유는 *Streptococcus mutans*와 *Escherichia coli*에 대해 농도 의존적인 항균 활성을 나타내었으며, 동시에 L929 섬유아세포와 MG63 조골세포 유사세포에 대해 높은 세포적합성을 유지하였다. 이상의 결과로부터 GmCP 나노섬유는 우수한 기계적 특성과 항균 성능을 세포적합성과 함께 갖춘 유망한 이중기능성 플랫폼으로서, 감염 저항성이 요구되는 치과용 조직유도재생 분야에 활용될 가능성이 있음을 확인하였다.

색인단어 : 키토산/폴리비닐알코올 나노섬유, 전기방사, 젠타마이신, 인장강도, 항균효과

Kyung Hee Park (ORCID ID: 0000-0002-7665-3580)
Yo-Han Song (ORCID ID: 0000-0001-7521-4757)
Alphonse Umugire (ORCID ID: 0000-0001-6515-5466)
Mi-Kyung Han (ORCID ID: 0000-0003-1434-1562)

*Correspondence: Yeong-Joon Park (ORCID ID: 0000-0003-0382-8535)
77, Yongbong-ro, Buk-gu, Gwangju 61186, Republic of Korea
Affiliation: Department of Dental Materials, School of Dentistry, Chonnam National University, Gwangju 61186, Korea
Tel: +82-62-530-4871, Fax: +82-62-530-4875
E-mail: yjpark@jnu.ac.kr

Received: Aug. 26, 2026; Revised: Sep. 16, 2026; Accepted: Sep. 16, 2026

Introduction

The guided tissue regeneration (GTR) technique uses membranes as a barrier to establish an isolated area around bone defects. This strategy provides an environment for bone regeneration while inhibiting the migration of epithelial cells into the bone-forming region (1, 2). In addition to serving as a physical barrier, GTR membranes should provide a suitable environment for tissue healing, as bacterial contamination at the surgical site may interfere with the regenerative process. Therefore, antibacterial functionality is an important consideration in the design of GTR membranes. Over the past decades, the biodegradable polymeric materials have become central to GTR strategies, enabling scaffolds to provide both structural support and controlled local delivery of therapeutic agents (3, 4). In particular, electrospun nanofibrous scaffolds have attracted growing attention due to their high surface area-to-volume ratio, interconnected porosity, and tunable architecture, all of which facilitate enhanced drug loading and favorable cellular interactions (5-7). Among biodegradable polymers, chitosan stands out as a natural polymer, biocompatible, and biodegradable material with intrinsic antibacterial activity (8, 9).

However, its practical application as a stand-alone material is often limited by poor mechanical strength and structural instability under physiological conditions. To address these limitations, chitosan is often blended with synthetic polymers such as poly(vinyl alcohol) (PVA), which enhances its mechanical properties through the formation of intermolecular and intramolecular hydrogen bonds (10). PVA also improves the processability of electrospinning and promotes hydrophilicity and cytocompatibility, making chitosan/PVA composite nanofibers a suitable platform for biomedical applications (11, 12). Recent advances have extended the role of such nanofibrous scaffolds by incorporating bioactive agents, antimicrobial peptides, anti-inflammatory drugs, and osteoinductive molecules to simultaneously promote regeneration and prevent infection (13-15). Among these agents, gentamicin (Gm), a broad-spectrum aminoglycoside antibiotic, is of particular interest due to its potent bactericidal activity and relatively low tendency to induce bacterial resistance (16). Gm exerts its antibacterial effects by electrostatic binding to ribosomes and disrupting protein synthesis, ultimately leading to bacterial cell death (17).

Although Gm-loaded electrospun nanofibers have been extensively explored for various biomedical applications, including ocular drug delivery, corneal repair, and wound healing, most studies have focused on polymer systems such as PVA/gelatin or PLA-based blends, while their application in periodontal or bone tissue regeneration remains limited and underexplored (16, 18, 19). Moreover, these studies often emphasize either antibacterial efficacy or drug release performance, without providing a comprehensive evaluation of mechanical strength, swelling behavior, and cytocompatibility, which are all critical for effective GTR membrane design.

To address these gaps, the present study aims to develop a dual-functional scaffold composed of chitosan and PVA, incorporating varying concentrations of gentamicin. By systematically varying the gentamicin concentration, we fabricated and characterized electrospun chitosan/PVA nanofibrous membranes in terms of morphology, thermal stability, swelling behavior, mechanical properties, antibacterial activity, and cytocompatibility. By optimizing Gm loading, we aimed to develop a bioactive scaffold that offers both mechanical robustness and localized antimicrobial efficacy, thereby demonstrating its potential as a multifunctional membrane for GTR applications.

Materials and Methods

1. Materials

Poly(vinyl alcohol) (PVA; 99% hydrolyzed, MW = 146,000 ~ 186,000 g · mol^{-1}), medium molecular weight chitosan, glacial acetic acid, and gentamicin sulfate solution (10 mg · mL^{-1} in deionized water) were purchased from Sigma-Aldrich (St. Louis, MO, USA). Acetic acid and phosphate-buffered saline (PBS, pH=7.4) were obtained from Gibco (Carlsbad, CA, USA).

2. Preparation of chitosan-PVA solution

An 8% (w/v) PVA solution was prepared by gradually dissolving 2.608 g of PVA in 30 mL of distilled water at 90 °C under continuous stirring until a clear, homogeneous solution was obtained. The solution was then cooled to room temperature. A 2% (v/v) acetic acid solution was prepared by adding 0.6 mL of glacial acetic acid to 29.4 mL of distilled water yielding a total volume of 30 mL. Subsequently, 0.612 g of chitosan (2 wt.% concentration) was dissolved in the acetic acid solution by stirring for 3 h at 70 °C. The chitosan and PVA solutions were then mixed in a 30 : 70 volume ratio and stirred for 2 h at room temperature to obtain the chitosan/PVA (CP) blend solution. Gentamicin solution was added to the CP solution with four different concentrations of 0.1%, 0.3%, 0.5%, and 1.0% (w/v), and the resulting GmCP solution mixtures were stirred for an additional 1 h at room temperature.

3. Electrospinning process

Electrospinning was conducted in an acrylic chamber, maintaining the relative humidity under 30% at 25 °C. The copolymer solution was loaded into a 10 mL plastic syringe fitted with a 23-gauge, 1/2-inch stainless steel needle. The solution was dispensed at a flow rate of 10 μL · min^{-1}, and a high voltage of 22 kV was applied between the needle and a grounded aluminum collector. The needle tip-to-collector distance was fixed at 15 cm. Electrospun nanofibers deposited onto the aluminum foil were carefully peeled off 7 h after the completion of electrospinning for further analysis.

4. Characterization of fibers

The surface morphology of the electrospun fibers was examined using a field emission scanning electron microscope (FE-SEM; S-4700, Hitachi, Tyoko, Japan) at 5,000× magnification. The average fiber diameter was determined by measuring 50 nanofibers at five different regions using ImageJ software (NIH Image, USA). The chemical interactions between chitosan/PVA and gentamicin were analyzed using attenuated total reflectance-Fourier transform infrared spectroscopy (ATR-FTIR, Perkin Elmer, Shelton, USA) by identifying the functional groups in the fibers at the range from 500 to 4000 cm^{-1}. The thermal stability of the CP and GmCP nanofibers was evaluated by thermogravimetric analysis system (TGA, Mettler Toledo, Greifensee, Switzerland) over a temperature range of 30-800 °C at a heating rate of 10 °C · min^{-1} under a nitrogen atmosphere with a flow rate of 50 mL · min^{-1}.

5. Mechanical properties

The mechanical properties of the CP and GmCP nanofibers were evaluated using a universal testing machine (Instron 4302, Instron Co., High Wyocombe, UK). Rectangular samples (40 mm × 10 mm) with thickness ranging from 0.25 to 0.33 mm were clamped using pneumatic grips with rubber-coated jaw faces. The grip distance was set to 20 mm, and tensile loading was applied at a crosshead speed of 10 mm · min^{-1} at room temperature (25 °C). Prior to testing, sample thicknesses were measured using a digital micrometer (Mitutoyo, Kawasaki, Japan). For each group, five specimens were tested. The mean and standard deviation of maximum tensile strength, Young's modulus, and % elongation at break were calculated. Statistical analysis was performed using nonparametric Kruskal-Wallis test, followed by Dunn's

multiple comparisons test, with a significance level set at $p < 0.05$.

6. Swelling test

The swelling behavior of the electrospun nanofiber mats was evaluated using phosphate-buffered saline (PBS, pH 7.4). Rectangular specimens weighing approximately 10 mg were cut from each sample, and their initial dry weights (W_{dry}) were recorded. The samples were immersed in 2 mL of PBS solution in a 6-well plate, and incubated at 37 ℃ for 24 h in a bio-oven at 150 rpm. After incubation, excess surface moisture was gently removed using filter paper, and the wet weight (W_{wet}) was measured. The swelling ratio (%) was calculated using the following equation (20):

$$\text{Swelling ratio}(\%) = \frac{W_{wet} - W_{dry}}{W_{dry}} \times 100$$

Where, W_{wet} and W_{dry} represent the weights of the hydrated and initial dry, respectively.

7. Antimicrobial assay

The antimicrobial activity of Gm-loaded chitosan/PVA (GmCP) nanofibers was evaluated using the Kirby-Bauer disc diffusion method (9, 21) against *Escherichia coli* (*E. coli*; KCTC 1682, Korean Collection for Type Cultures) and *Streptococcus mutans* (*S. mutans*; ATCC 25175, American Type Culture Collection). *S. mutans* was cultured on brain heart infusion (BHI) agar and broth at 37 ℃ for 24 h, and *E. coli* was cultured on nutrient agar and broth under the same conditions. Bacterial suspensions were adjusted to a concentration of 1×10^7 CFU · mL^{-1} based on optical density measurements. A volume of 70 μL of each suspension was evenly spread on BHI agar plates for *S. mutans* and nutrient agar plates for *E. coli*. Disc-shaped samples (10 mm in diameter) were cut from Gm-loaded and unloaded nanofiber mats and sterilized under UV light for 60 min in a laminar flow cabinet. After sterilization, the discs were placed directly onto the inoculated agar plates. Nanofiber mats without gentamicin (0% Gm) served as the control group. All plates were incubated at 37 ℃ for 24 h in a CO_2 incubator. Following incubation, inhibition zones-defined as clear halos surrounding the discs indicating suppressed bacterial growth-were photographed and measured using ImageJ software (NIH Image, Bethesda, USA). The experiment was repeated five times (n=5).

8. Cell viability test

For the cell viability assay, L929 (National Collection of Type Cultures [NCTC] clone 929)) and MG63 (Korean Cell Line Bank, KCLB No. 21327) cells were seeded in 12-well plate at a density of 1×10^5 cells per well and incubated for 24 h. Electrospun nanofiber samples containing different concentrations of gentamicin (0%, 0.1%, 0.3%, 0.5%, and 1.0%) were rinsed with PBS and placed into Transwell inserts (SPL Life Science, Pocheon, Korea). Subsequently, these hanging inserts containing the samples were positioned atop the cells cultivated in a 12-well plate. One milliliter of culture medium was added to each well to fully submerge the nanofibers, followed by a 24-hour co-cultivation with the cells. After incubation, the culture medium was removed, and the cells were washed with PBS. A solution of MTT (0.5 mg · mL^{-1}; Amresco, Solon, USA) was added to each well and incubated for 2 h. After removing the MTT solution, the resulting formazan crystals were dissolved in dimethyl sulfoxide (DMSO) for 15 min. Absorbance was measured at 570 nm using a microplate reader (Tecan, Männedorf, Switzerland), and cell viability was calculated relative to the control group. Cells cultured in medium without nanofiber samples served as the control group. The experiment was repeated three times (n = 3).

Results

1. Morphology of electrospun nanofibers

Figure 1 shows the morphology and average fiber diameters of electrospun chitosan/PVA (CP) nanofibers containing gentamicin at increasing concentrations (0%, 0.1%, 0.3%, 0.5%, and 1.0%). All groups exhibited uniform, bead-free nanofibrous structures without visible defects or broken fibers observed in any group.

The average fiber diameters were 162 ± 15 nm, 199 ± 29 nm, 209 ± 41 nm, 203 ± 38 nm, and 157 ± 25 nm for the 0%, 0.1%, 0.3%, 0.5%, and 1.0% Gm groups, respectively (Figure 1f). The fiber diameter varied across the different Gm concentrations, with the highest mean diameter (209 ± 41 nm) observed in the 0.3% Gm group. At 1.0% Gm, the mean fiber diameter decreased to 157 ±

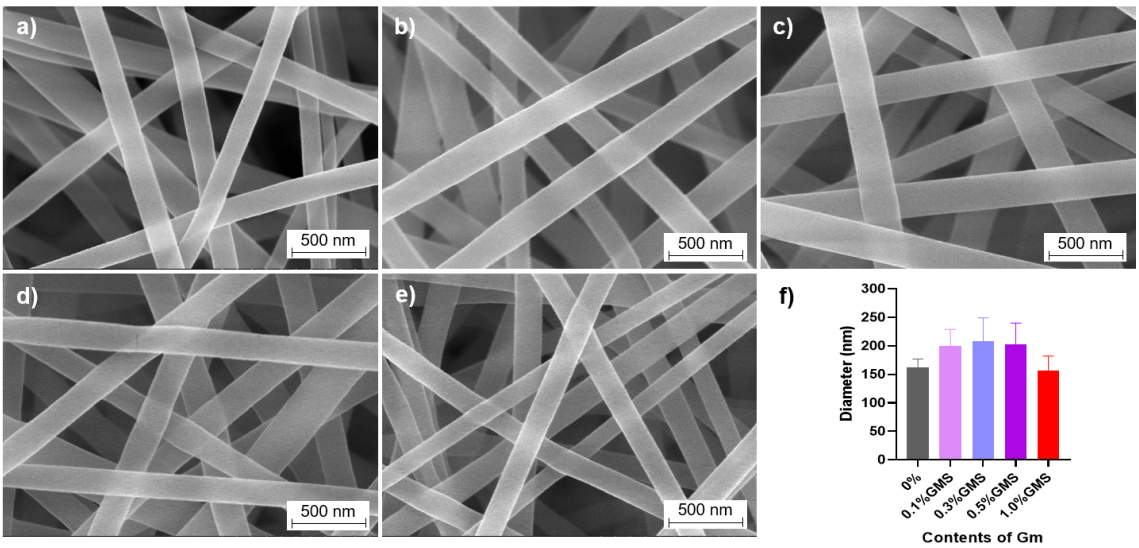


Figure 1. SEM images of electrospun chitosan/PVA (CP) nanofibers containing different concentrations of gentamicin (Gm): a) 0%, b) 0.1%, c) 0.3%, d) 0.5%, and e) 1.0%. All nanofibers exhibit smooth, bead-free morphology. The mean and S.D. values of the nanofiber diameters are presented in f). n = 50 fibers per each group.

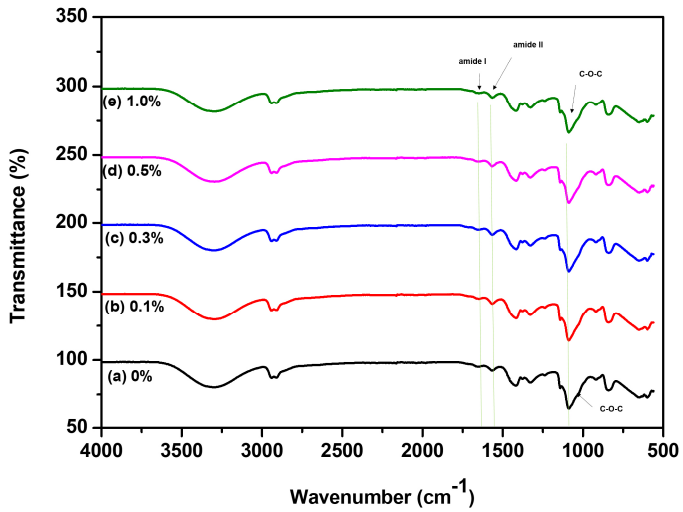


Figure 2. FT-IR spectra of electrospun chitosan/PVA nanofibers loaded with different concentrations of gentamicin: a) 0 %, b) 0.1%, c) 0.3%, d) 0.5%, and e) 1.0%.

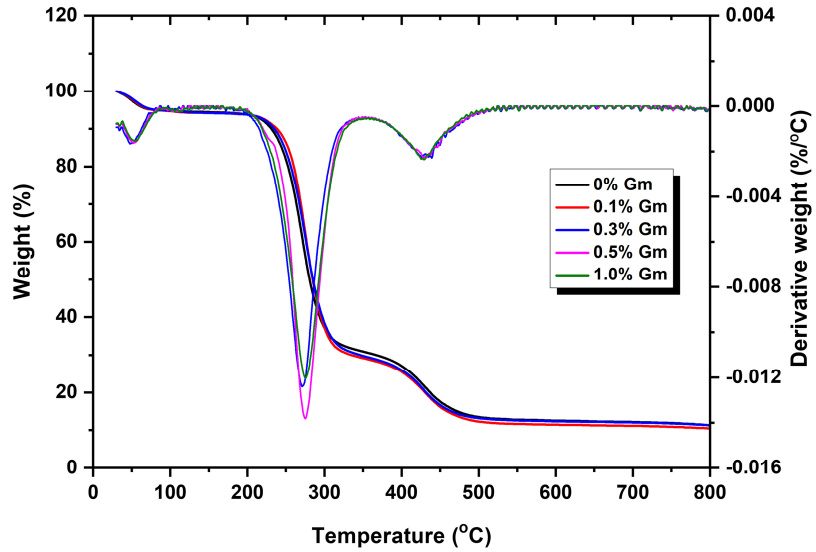


Figure 3. TGA and DTG thermograms of electrospun chitosan/PVA nanofibers loaded with different concentrations of gentamicin (0%, 0.1%, 0.3%, 0.5%, and 1.0%). Gm denotes gentamicin sulfate solution (10 mg · mL^{-1} in deionized water).

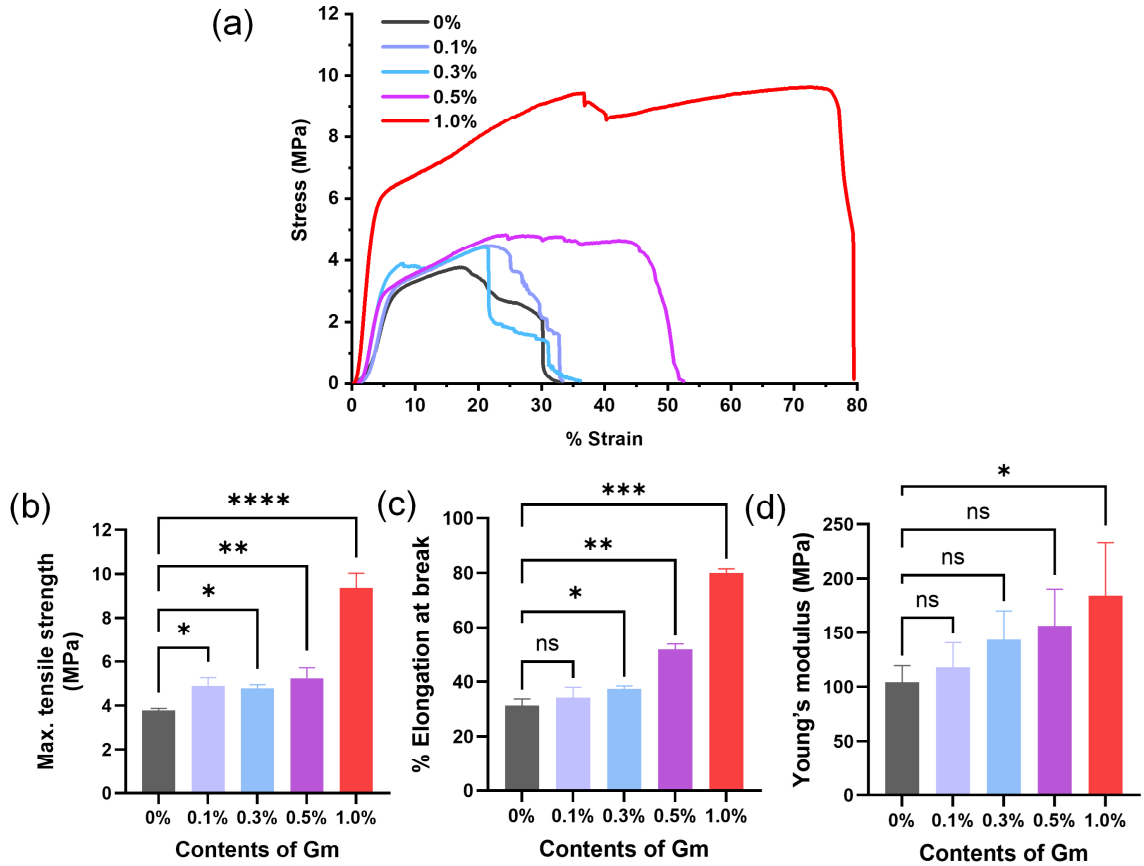


Figure 4. Mechanical properties of electrospun chitosan/PVA nanofiber mats loaded with varying concentrations of gentamicin: (a) representative strain-stress curves, (b) maximum tensile strength, (c) % elongation at break, and (d) Young's modulus. Data are presented as mean ± standard deviation. *p 〈 0.05, ** p 〈 0.01, *** p 〈 0.001, and **** p 〈 0.0001 (statistical significance). n = 5 replicates for each group.

25 nm, which was comparable to that of the unloaded group.

2. ATR-FTIR analysis

Figure 2 presents the ATR-FTIR spectra of electrospun CP and gentamicin-loaded CP (GmCP) nanofibers with varying Gm concentrations. The unloaded CP nanofibers (Figure 2a) exhibited a broad absorption band at 3298 cm^{-1}, corresponding to O-H stretching vibrations, and a characteristic peak at 2911 cm^{-1} attributed to C-H stretching vibrations. Additional absorption bands were observed near 1650 cm^{-1} and 1550 cm^{-1}, as well as in the fingerprint region between 1000 and 1200 cm^{-1}. The spectra of the Gm-loaded nanofibers (Figure 2b-e) displayed similar absorption bands to those observed in the unloaded CP nanofibers. The broad band around 3298 cm^{-1} and the peak near 2911 cm^{-1} were present in all groups. The absorption bands near 1650 cm^{-1} and 1550 cm^{-1} were also retained after gentamicin incorporation. In addition, a slight shift of the band located near 1150 cm^{-1} in the unloaded CP nanofibers to approximately 1155 cm^{-1} was observed in the Gm-loaded groups. No new major absorption bands were detected following gentamicin incorporation, and the overall spectral profiles remained similar among all samples.

3. Thermal stability

The TGA and DTG thermograms of electrospun CP and GmCP nanofibers (0.1% - 1.0% gentamicin) are presented in Figure 3. Similar thermal degradation profiles were

Table 1. Mechanical properties of electrospun chitosan/PVA nanofiber mats loaded with varying concentrations of gentamicin (n = 5)

Gentamicin solution content (%)	Stress at maximum load (MPa)	Young's modulus (MPa)	% elongation at break (%)
0 (Ctrl)	3.8 (0.1)^{a,*}	104.3 (12.4)^{a}	31.3 (2.0)^{a}
0.1	4.9 (0.4)^{b}	118.1 (18.5)^{a}	34.2 (3.1)^{a,b}
0.3	4.8 (0.2)^{b}	143.3 (22.0)^{a}	37.4 (0.9)^{b}
0.5	5.2 (0.5)^{c}	156.5 (27.7)^{a,b}	51.9 (1.6)^{c}
1.0	9.4 (0.7)^{d}	184.5 (39.6)^{b}	80.1 (1.2)^{d}

*Different small lowercase letters indicate significant differences between groups at $p < 0.05$, with n = 5 replicates per each group.

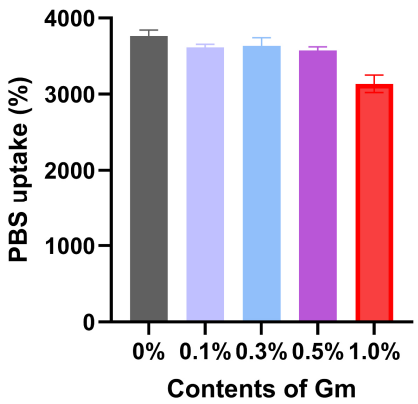


Figure 5. Phosphate-buffered saline (PBS) uptake of electrospun chitosan/PVA nanofiber mats loaded with different concentrations of gentamicin (n = 5). Gm denotes gentamicin sulfate solution (10 $mg \cdot mL^{-1}$ in deionized water).

observed across all experimental groups, with each consistently revealing three major stages of weight loss. The initial weight loss occurred between approximately 35 and 85 °C, with a mass loss of 5.5–6.0% corresponding to the evaporation of residual moisture. The second stage occurred between approximately 200 and 330 °C, resulting in a major weight loss of 63–65%. The third degradation stage was observed between approximately 380 and 490 °C with an additional weight loss of approximately 18%. Complete degradation occurred at approximately 544 °C for CP and 563 °C for GmCP, respectively, with a small amount of residual mass values ranging from 11.1% to 14.7% for GmCP nanofibers and 12.5% for CP nanofibers.

4. Mechanical properties

Representative stress–strain curves are shown in Figure 4a, and the quantitative mechanical properties are summarized in Table 1. The maximum tensile strength increased from 3.8 ± 0.1 MPa in the unloaded CP group to 9.37 ± 0.70 MPa in the 1.0% Gm group (Figure 4b), Similarly, Young's modulus increased from 104.3 MPa in the unloaded group to 184.5 MPa in the 1.0% Gm group (Figure 4d). The maximum % elongation at break increased from 31.3 ± 2.0% to 80.1 ± 1.2% with increasing gentamicin concentration (Figure 4c, Table 1). Statistically significant differences were observed between the unloaded and gentamicin-loaded groups, as indicated in Figure 4.

5. Swelling behavior

The PBS uptake of electrospun chitosan/PVA (CP) nanofiber mats containing different concentrations of gentamicin after 24 h of immersion is presented in Figure 5. All groups exhibited high PBS absorption capacity, with swelling ratios exceeding 3000%.

The unloaded CP nanofibers (0% Gm) exhibited the highest swelling ratio, reaching approximately 3700%. Following gentamicin incorporation, a gradual decrease in PBS uptake was observed. The 0.1%, 0.3%, and 0.5% Gm-loaded nanofibers showed comparable swelling ratios, ranging from approximately 3550% to 3650%. The lowest swelling ratio was observed in the 1.0% Gm group, which exhibited a PBS uptake of approximately 3100%. In general, PBS uptake decreased as gentamicin concentration increased, with the most pronounced reduction observed at 1.0% Gm loading.

6. Antibacterial activity

The antimicrobial activity of GmCP nanofiber mats was evaluated by measuring the diameter of the bacterial inhibition zones. Figure 6 illustrates the antibacterial activity of GmCP nanofiber mats against *S. mutans* and *E. coli*. No noticeable inhibition zones were observed in the control group (0% Gm), indicating minimal antimicrobial activity of the CP nanofiber mats in the absence of gentamicin. For *S. mutans* (Figure 6a), the inhibition zone diameters were 8.8 ± 0.4 mm, 10.4 ± 0.4 mm, and 13.9 ± 0.6 mm for Gm concentrations of 0.3%, 0.5%, and 1.0%, respectively.

In the case of *E. coli* (Figure 6b), antibacterial activity was also enhanced with increasing Gm concentration. The corresponding inhibition zone diameters were 9.3 ± 0.6 mm, 12.0 ± 1.2 mm, 12.7 ± 0.9 mm, and 16.2 ± 0.8 mm for 0.1%, 0.3%, 0.5%, and 1.0% GmCP nanofiber mats, respectively. These quantitative results are summarized in Table 2. The inhibition-zone diameter increased with increasing gentamicin concentration for both bacterial strains.

7. Cell viability

Figure 7 presents the viability of L929 fibroblasts (Figure 7a) and MG63 osteoblast-like cells (Figure 7b) cultured in the presence of gentamicin-loaded chitosan/PVA (GmCP) nanofiber mats containing 0%, 0.1%, 0.3%, 0.5%, and 1.0% gentamicin after 24 h of incubation. For L929 fibroblasts, all groups exhibited cell viability above 80%. A slight increase in viability was observed following gentamicin incorporation, with the highest viability detected in the 0.3% Gm group. However, no statistically significant differences were

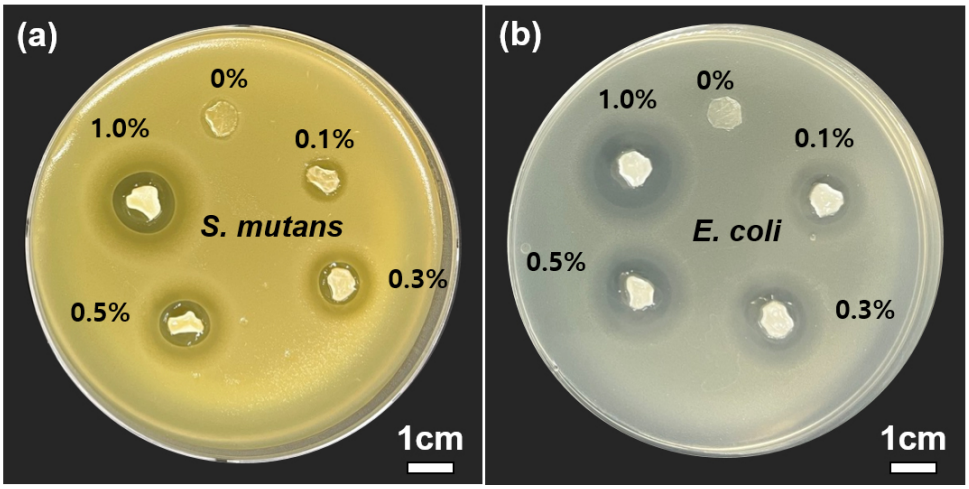


Figure 6. Antibacterial activity of electrospun chitosan/PVA nanofibers loaded with varying concentrations of gentamicin against (a) *S. mutans* and (b) *E. coli*.

Table 2. Zone of inhibition (mm) indicating the antibacterial activity of electrospun chitosan/PVA nanofiber mats loaded with varying concentrations of gentamicin against *S. mutans* and *E. coli* after 1 day (n = 5)

Content of Gm (%)	Zone of inhibition (mm)	
	S. mutans	*E. coli*
0 (Ctrl)	0	0
0.1	0	9.3 (0.6)
0.3	8.8 (0.4)	12.0 (1.2)
0.5	10.4 (0.4)	12.7 (0.9)
1.0	13.9 (0.6)	16.2 (0.8)

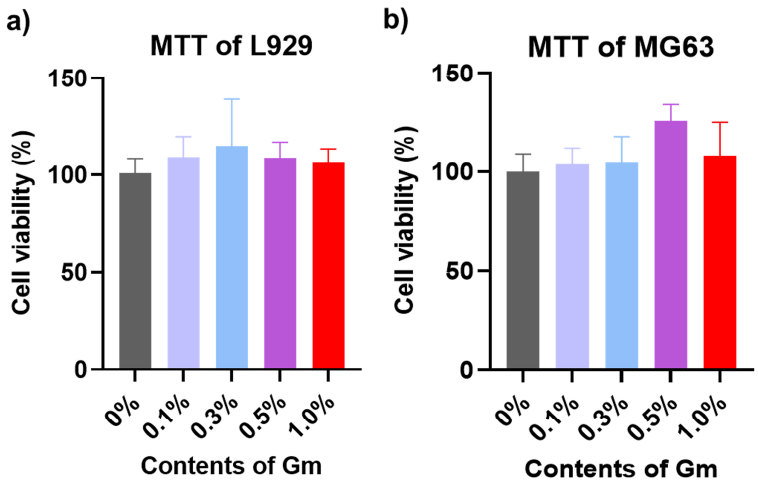


Figure 7. Cell viability of electrospun chitosan/PVA nanofiber mats loaded with varying concentrations of gentamicin, assessed by MTT assay for (a) L929 fibroblasts and (b) MG63 osteoblast-like cells. Data are presented as mean ± standard deviation (n = 3).

observed among the groups ($p > 0.05$).

Similarly, all MG63 cells maintained viability above 80% after exposure to the nanofiber mats. The 0.5% Gm group exhibited the highest cell viability among all tested concentrations, whereas the remaining groups showed viability values comparable to the unloaded CP nanofibers. No statistically significant differences were observed between the gentamicin-loaded groups and the control group ($p > 0.05$). All GmCP nanofiber formulations maintained high cell viability in both L929 fibroblasts and MG63 osteoblast-like cells after 24 h of incubation.

Discussion

The incorporation of gentamicin influenced the morphology of electrospun chitosan/PVA nanofibers while maintaining smooth, uniform, bead-free structures without any broken strands (Figure 1). Fiber diameter showed a non-monotonic variation with increasing gentamicin concentration, with an increase at lower concentrations and a decrease at 1.0% Gm. These changes may be associated with alterations in the physicochemical properties of the spinning solution and intermolecular interactions among gentamicin, chitosan, and PVA, which could influence polymer chain entanglement and alter the stretching behavior of the polymer jet during electrospinning. Similar effects have been reported in drug-loaded electrospun systems, where modifications in solution conductivity and polymer interactions affected fiber formation and morphology (10, 22, 23).

ATR-FTIR analysis indicated that gentamicin incorporation did not substantially alter the characteristic chemical structure of the chitosan/PVA matrix (Figure 2). The preservation of the major characteristic absorption bands across all groups suggests that no major chemical changes occurred in the polymer matrix following gentamicin incorporation. The minor spectral shifts observed after gentamicin loading may indicate secondary interactions between gentamicin and the polymer chains. Such interactions are likely associated, at least in part, with hydrogen bonding involving hydroxyl and amino groups in PVA, chitosan, and gentamicin. Similar hydrogen-bonding interactions between PVA and chitosan have been reported in chitosan/PVA nanofibers, while gentamicin-loaded PVA/chitosan nanofibers have also shown FTIR changes consistent with intermolecular interactions between gentamicin and the polymer matrix (23, 24).

The thermal degradation profiles of the CP and GmCP nanofibers exhibited similar degradation patterns, indicating that gentamicin incorporation did not substantially alter the thermal behavior of the chitosan/PVA matrix (Figure 3). Similar thermal degradation behavior has been reported for electrospun chitosan/PVA-based membranes (25). Comparable thermal degradation behavior has also been reported for drug-loaded PVA/chitosan nanofibers (26), and particularly in gentamicin-loaded PVA/chitosan nanofiber membranes (23). These findings support the observed preservation of the overall thermal stability of the polymer matrix following gentamicin incorporation, demonstrating that gentamicin loading did not compromise the thermal resistance of the polymer matrix. This finding suggests that the antibiotic was successfully incorporated without disrupting the overall polymer network structure (26).

Mechanical stability is an important requirement for guided tissue regeneration membranes because the membranes must maintain their structural integrity while withstanding mechanical stresses during the healing period. The improvement in tensile properties observed with increasing gentamicin concentration suggests that gentamicin incorporation contributed to reinforcement of the chitosan/PVA nanofibrous matrix. These enhancements may be associated with altered intermolecular interactions among PVA, chitosan and gentamicin, which could contribute to the observed improvement in the mechanical properties of the nanofibrous matrix (23, 27, 28).

Importantly, the simultaneous increase in tensile strength

and elongation at break indicates that gentamicin incorporation enhanced both the mechanical strength and flexibility of the scaffold (Figure 4, Table 1). Such a combination of properties is advantageous for GTR applications, where membranes must maintain mechanical stability while remaining sufficiently flexible for clinical handling and adaptation to irregular defect geometries (1, 27).

Water uptake of tissue-engineering scaffolds is an important characteristic because it can influence nutrient transport, drug release, and cellular interactions. The reduction in swelling behavior following gentamicin incorporation suggests the formation of a denser polymer network with reduced accessibility to water molecules (Figure 5). Similar effects have been reported for chitosan/PVA-based nanofibrous systems, where polymer composition and intermolecular interactions influence water uptake and matrix swelling (22, 27).

The amino groups of chitosan are known to contribute significantly to hydrophilicity through hydrogen bonding with water. Interactions between gentamicin and these functional groups may reduce the number of available hydrophilic sites and consequently decrease water absorption. In addition, enhanced intermolecular interactions between the polymer chains may restrict matrix expansion during hydration. Similar reductions in swelling have been reported in drug-loaded chitosan/PVA systems where increased molecular interactions contributed to greater structural compactness (23, 26). For GTR applications, appropriate swelling behavior is desirable because the membrane should maintain its dimensional and mechanical integrity while permitting adequate hydration and transport of biologically relevant molecules (1, 6).

Bacterial contamination is an important concern in periodontal and bone regenerative procedures, and incorporation of antimicrobial agents into barrier membranes has become an attractive strategy for improving regenerative outcomes (1, 6). Gentamicin is a broad-spectrum aminoglycoside antibiotic that exerts bactericidal activity primarily by interfering with bacterial protein synthesis through interaction with the bacterial ribosome (16). The antibacterial activity observed in the gentamicin-loaded nanofibers demonstrates the antimicrobial functionality of the GmCP membranes. The concentration-dependent increase in inhibition-zone diameter suggests that increasing gentamicin loading enhanced the antibacterial activity of the nanofibrous membranes (Figure 6, Table 2). However, because quantitative gentamicin-release kinetics were not evaluated in the present study, these antibacterial results cannot be used to establish a controlled or localized gentamicin-release profile. The antibacterial activity against both *S. mutans* and *E. coli* further demonstrates the broad antibacterial performance of the GmCP nanofibers against representative Gram-positive and Gram-negative bacteria. These findings suggest that gentamicin-loaded chitosan/PVA nanofibers may have potential for providing antimicrobial functionality in GTR membranes, particularly during the early stages of tissue regeneration (1, 6, 9, 18). Further studies are required to determine the gentamicin-release kinetics and duration of antimicrobial activity under physiologically relevant conditions and correlate the release profile with antibacterial activity over time. In addition, the biodegradation behavior of the chitosan/PVA nanofibrous membranes was not quantitatively evaluated. Therefore, future studies should investigate membrane degradation behavior to better assess their long-term suitability for GTR applications.

An ideal GTR membrane should provide antimicrobial activity without inducing cytotoxic effects on surrounding host tissues (1, 6). The maintenance of high cell viability in both L929 fibroblast and MG63 osteoblast-like cells indicates that gentamicin incorporation did not adversely affect the biocompatibility of the nanofibrous scaffold (Figure 7).

The favorable cellular response is consistent with the well-established biocompatibility of chitosan/PVA-based nanofibrous scaffolds for tissue-engineering applications.

Chitosan and PVA possess complementary properties, including hydrophilicity, processability, and mechanical stability, which contribute to their application in biomedical scaffolds (22, 24, 25).

The present findings further indicate that the gentamicin concentrations investigated maintained high cell viability while providing antibacterial activity. Similar multifunctional behavior has been reported for drug-loaded PVA/chitosan nanofibrous systems (18, 23).

The favorable response of MG63 osteoblast-like cells is particularly encouraging because osteoblastic activity is essential for bone regeneration in periodontal defects. Together with the favorable response observed in L929 fibroblasts, these findings support the potential of gentamicin-loaded chitosan/PVA nanofibers as multifunctional membranes combining antibacterial activity with cellular compatibility for GTR applications (1, 6, 22, 29).

Conclusion

Chitosan-PVA nanofiber mats loaded with varying concentrations of gentamicin (GmCP) were successfully fabricated via electrospinning, yielding uniform, bead-free, randomly aligned nanofibers with diameters ranging from approximately 162 nm to 209 nm. FT-IR and TGA analyses confirmed that the incorporation of gentamicin did not compromise the structural integrity or thermal stability of the polymer matrix. Mechanical testing revealed that increasing Gm content enhanced both tensile strength and ductility, while simultaneously reducing the PBS swelling ratio, likely due to increased intermolecular interactions. GmCP nanofiber mats exhibited antibacterial activity against *E. coli* and *S. mutans*, while maintaining high cytocompatibility with L929 fibroblasts and MG63 osteoblast-like cells. These multifunctional properties suggest that gentamicin-loaded chitosan/PVA nanofiber mats are promising candidates for infection-resistant and biocompatible scaffolds for guided tissue regeneration applications. However, further studies involving quantitative gentamicin-release kinetics, biodegradation assessment, and mechanical evaluation using larger sample sizes are necessary to validate their long-term performance and further establish their suitability for GTR applications.

Acknowledgements

This work was supported by the National Research Foundation of Korea (NRF) grant funded by the Korea government (MSIT) (NRF-2019R1A5A2027521) and by Ministry of Education (No. NRF-2021R1I1A1A01055994).

References

1. Ul Hassan S, Bilal B, Nazir MS, Naqvi SAR, Ali Z, Nadeem S, et al. Recent progress in materials development and biological properties of GTR membranes for periodontal regeneration. Chem Biol Drug Des. 2021;98(6):1007-25.
2. Mukherjee C, Varghese D, Krishna J, Boominathan T, Rakeshkumar R, Dineshkumar S, et al. Recent advances in biodegradable polymers—properties, applications and future prospects. Eur Polym J. 2023;192:112068.
3. Serrano-Aroca Á, Cano-Vicent A, i Serra RS, El-Tanani M, Aljabali A, Tambuwala MM, et al. Scaffolds in the microbial resistant era: Fabrication, materials, properties and tissue engineering applications. Mater Today Bio. 2022;16:100412.
4. Hiwrale A, Bharati S, Pingale P, Rajput A. Nanofibers: A current era in drug delivery system. Heliyon. 2023;9(9):e19642.
5. Alavarse AC, de Oliveira Silva FW, Colque JT, da Silva VM, Prieto T, Venancio EC, et al. Tetracycline hydrochloride-loaded electrospun nanofibers mats based

on PVA and chitosan for wound dressing. Mater Sci Eng C Mater Biol Appl. 2017;77:271-281.
6. Zhao P, Chen W, Feng Z, Liu Y, Liu P, Xie Y, et al. Electrospun nanofibers for periodontal treatment: a recent progress. Int J Nanomedicine. 2022;17:4137-4162.
7. Gaydhane MK, Sharma CS, Majumdar S. Electrospun nanofibres in drug delivery: advances in controlled release strategies. RSC Adv. 2023;13(11):7312-7329.
8. Adhikari J, Ghosh M, Das P, Basak P, Saha P. Polycaprolactone assisted electrospinning of honey/betel with chitosan for tissue engineering. Mater Today Proc. 2022;57:307-313.
9. Monteiro N, Martins M, Martins A, Fonseca NA, Moreira JN, Reis RL, et al. Antibacterial activity of chitosan nanofiber meshes with liposomes immobilized releasing gentamicin. Acta Biomater. 2015;18:196-207.
10. Cheng Y, Far BF, Jahanbakhshi M, Bahrami S, Tamimi P, Sedaghat M, et al. Exploring the potential of a polyvinyl alcohol/chitosan-based nanofibrous matrix for erythromycin delivery: fabrication, in vitro and in vivo evaluation. RSC Adv. 2023;13(27):18450-18459.
11. Madani F, Mujokoro B, Mohammadi S, Khosravani M, Adabi M. Chitosan/PVA nanofibers for implantable drug delivery systems. Nanomed Res J. 2022;7(2):150-159.
12. Park JH, Lee HW, Chae DK, Oh W, Yun JD, Deng Y, et al. Electrospinning and characterization of poly (vinyl alcohol)/chitosan oligosaccharide/clay nanocomposite nanofibers in aqueous solutions. Colloid Polym Sci. 2009;287(8):943-951.
13. Omidian H, Gill EJ. Nanofibrous scaffolds in biomedicine. J Compos Sci. 2024;8(7):269.
14. Yan B, Zhang Y, Li Z, Zhou P, Mao Y. Electrospun nanofibrous membrane for biomedical application. SN Appl Sci. 2022;4(6):174.
15. Jain N, Jain GK, Javed S, Iqbal Z, Talegaonkar S, Ahmad FJ, et al. Recent approaches for the treatment of periodontitis. Drug Discov Today. 2008;13(21-22):932-943.
16. Athauda I, Shetty M, Pai P, Hegde M, Gurumurthy S, Babitha K. Enhanced bactericidal effects and drug delivery with gentamicin-conjugated nanoparticles. J Cluster Sci. 2024;35(2):371-382.
17. Michalska-Sionkowska M, Baczmarek B, Walczak M, Sionkowska A. Antimicrobial activity of new materials based on the blends of collagen/chitosan/hyaluronic acid with gentamicin sulfate addition. Mater Sci Eng C Mater Biol Appl. 2018;86:103-109.
18. Cesur S, Ilhan E, Tut TA, Kaya E, Dalbayrak B, Bosgelmez-Tinaz G, et al. Design of cinnamaldehyde-and gentamicin-loaded double-layer corneal nanofiber patches with antibiofilm and antimicrobial effects. ACS Omega. 2023;8(31):28109-28124.
19. Mirzaeei S, Taghe S, Asare-Addo K, Nokhodchi A. Polyvinyl alcohol/chitosan single-layered and polyvinyl alcohol/chitosan/eudragit rl100 multi-layered electrospun nanofibers as an ocular matrix for the controlled release of ofloxacin: An in vitro and in vivo evaluation. AAPS PharmSciTech. 2021;22(5):170.
20. Guadalupe E, Ramos D, Shelke NB, James R, Gibney C, Kumbar SG. Bioactive polymeric nanofiber matrices for skin regeneration. J Appl Polym Sci. 2015;132(16):41850.
21. Hudzicki J. Kirby-Bauer disk diffusion susceptibility test protocol. Am Soc Microbiol. 2009;15(1):1-23.
22. Al-Madhagy G, Alghoraibi I, Darwich K, Hajeer MY, Al-Madhagy GM. Evaluation of the chemical, morphological, physical, mechanical, and biological properties of chitosan/polyvinyl alcohol nanofibrous scaffolds for potential use in oral tissue engineering. Cureus. 2022;14(10):e30374.
23. Mustafa FE, Lee BK. Improved mechanical stability and regulated gentamicin-release of polyvinyl alcohol/chitosan nanofiber membranes via heat treatment. J Biomed Mater Res A. 2025;113(4):e37905.
24. Olvera Bernal RA, Olekhnovich RO, Uspenskaya MV. Chitosan/PVA nanofibers as potential material for the

development of soft actuators. Polymers. 2023;15(9): 2037.
25. Sánchez-Machado DI, López-Cervantes J, Vega-Cázarez CA, Hernández-Ruiz KL, Campas-Baypoli ON, Soto-Cota A, et al. Functional and antibacterial characterization of electrospun nanofiber membranes made of chitosan and polyvinyl alcohol. Results Chem. 2024;7:101314.
26. Alotaibi BS, Khan AK, Kharaba Z, Yasin H, Yasmin R, Ijaz M, et al. Development of poly (vinyl alcohol)–Chitosan composite nanofibers for dual drug therapy of wounds. ACS Omega. 2024;9(11):12825-12838.
27. Salleh NAM, Afifi AM, Zuki FM, SalehHudin HS. Enhancing mechanical properties of chitosan/PVA electrospun nanofibers: a comprehensive review. Beilstein J Nanotechnol. 2025;16(1):286-302.
28. Bonilla J, Fortunati E, Atarés L, Chiralt A, Kenny JM. Physical, structural and antimicrobial properties of poly vinyl alcohol–chitosan biodegradable films. Food Hydrocoll. 2014;35:463-470.
29. Pineda-Castillo S, Bernal-Ballén A, Bernal-López C, Segura-Puello H, Nieto-Mosquera D, Villamil-Ballesteros A, et al. Synthesis and characterization of poly(vinyl alcohol)-chitosan-hydroxyapatite scaffolds: a promising alternative for bone tissue regeneration. Molecules. 2018;23(10):2414.

Research Article

Fabrication of gentamicin-loaded chitosan/polyvinyl alcohol electrospun nanofibrous dual-functional scaffolds for guided tissue regeneration

*Kyung Hee Park, Yo-Han Song, Alphonse Umugire, Mi-Kyung Han, Yeong-Joon Park**

Department of Dental Materials, School of Dentistry,
Chonnam National University, Gwangju, Republic of Korea

This study presents the effect of compositional variations of electrospun nanofibrous mats composed of chitosan and polyvinyl alcohol (PVA), incorporated with varying concentrations of gentamicin (Gm), as multifunctional scaffolds for guided tissue regeneration (GTR). The Gm-loaded chitosan/PVA nanofibers (GmCP) were systematically evaluated for their morphology, thermal stability, swelling behavior, mechanical properties, antibacterial activity, and cytocompatibility. Gentamicin incorporation did not affect the structural or thermal stability of the GmCP nanofibers. Notably, increasing Gm concentrations up to 1.0% (w/v) led to improved mechanical properties of the mats, with improvements in tensile strength, Young's modulus, and percent elongation at break. These enhancements may be associated with altered intermolecular interactions among PVA, chitosan, and gentamicin, which could contribute to the observed improvement in mechanical properties. The swelling ratio decreased with increasing Gm content which may be associated with changes in intermolecular interactions within the chitosan/PVA matrix, that could influence water accessibility and matrix expansion. Antibacterial assays showed that GmCP nanofibers exhibited dose-dependent antibacterial activity against *Streptococcus mutans* and *Escherichia coli*, while maintaining high cytocompatibility with L929 fibroblasts and MG63 osteoblast-like cells. These results suggest that GmCP nanofibers provide a promising dual-function platform — combining mechanical robustness and antibacterial performance with cytocompatibility — for potential infection-resistant, guided tissue-regenerative dental applications.

Keywords : chitosan nanofiber, electrospinning, gentamicin, tensile strength, antibacterial effect